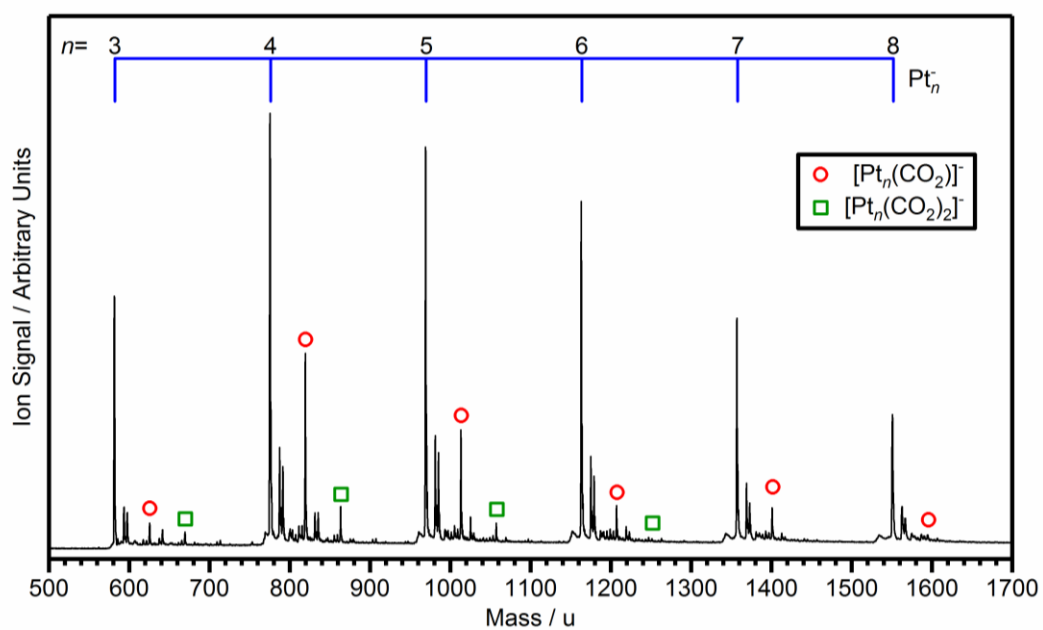


## Table of Contents

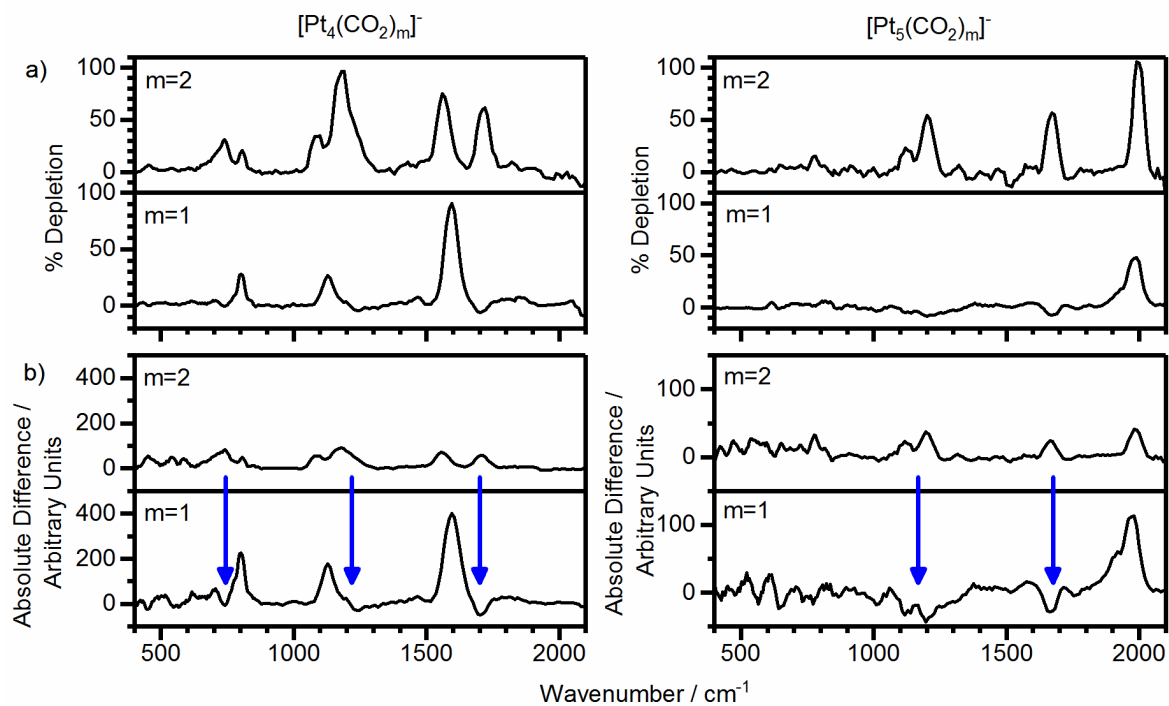
1. Time-of-Flight Mass Spectrum .....	2
2. IR-MPD of $[\text{Pt}_n(\text{CO}_2)_2]^-$ Clusters .....	3
3. Fragmentation of $[\text{Pt}_n(\text{CO}_2)_2]^-$ , $[\text{Pt}_n\text{O}(\text{CO}_2)_2]^-$ and $[\text{Pt}_n(\text{CO}_2)]^-$ Clusters.....	4
4. Details of the Computational Methodology Employed .....	5
5. Calculated Energetically Low-Lying Structures of $\text{Pt}_4^-$ .....	6
6. Calculated Energetically Low-Lying Structures of $\text{Pt}_5^-$ .....	7
7. Simulated IR Spectra of Low-Lying $[\text{Pt}_4(\text{CO}_2)]^-$ Structures .....	8
8. Simulated IR Spectra of Low-Lying $[\text{Pt}_5(\text{CO}_2)]^-$ Structures .....	9
9. Details of Key Structures.....	10
10. Calculated $\text{Pt}_4^- + \text{CO}_2$ Reactive Potential Energy Surface .....	11
11. Calculated Energetically Low-Lying Structures of $[\text{Pt}_n(\text{CO}_2)]^-$ ( $n=1-3$ ) .....	12
12. Charge Distribution Analysis of Key Structures.....	13

## 1. Time-of-Flight Mass Spectrum



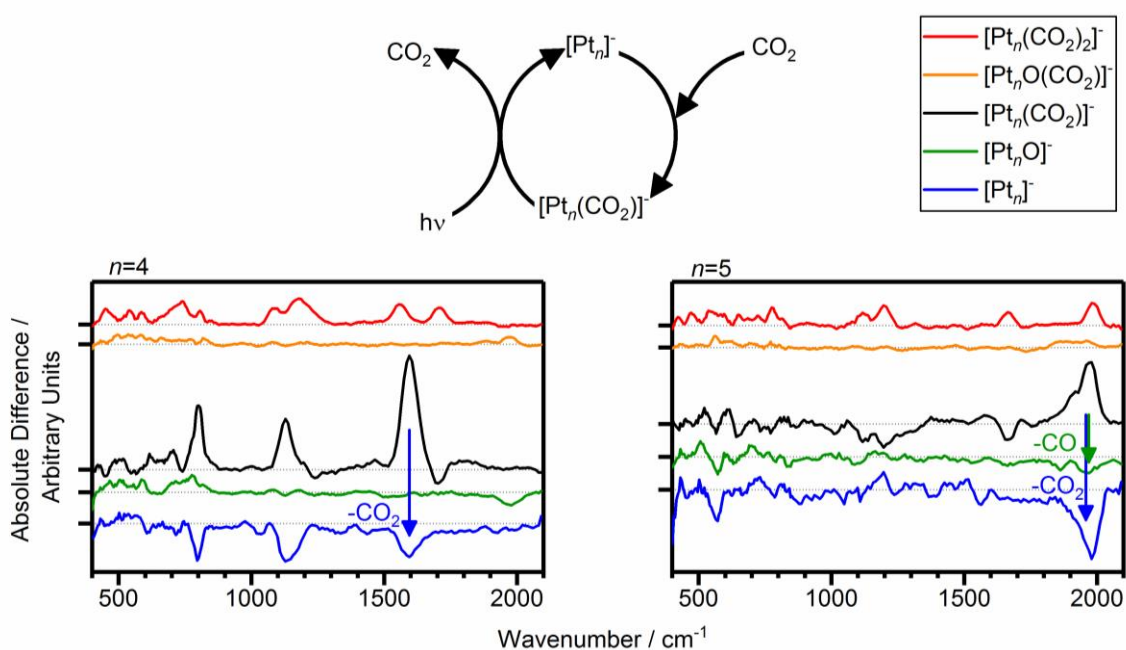
**Figure S1.** Time-of-Flight mass spectrum obtained following laser ablation of a <sup>194</sup>Pt enriched platinum target in the presence of a carrier gas of helium and reaction gas of CO<sub>2</sub>.

## 2. IR-MPD of $[\text{Pt}_n(\text{CO}_2)_2]^-$ Clusters



**Figure S2.** IR-MPD spectra of  $[\text{Pt}_n(\text{CO}_2)_m]^-$  ( $n=4$  or  $5$  and  $m=1$  or  $2$ ) clusters in the spectral region  $400\text{--}2100\text{ cm}^{-1}$ . Depletion is given as a) a percentage and b) an absolute difference. The small dips (enhancements) in the spectra of  $m=1$  match well with the position of depletions observed in the spectra of the corresponding larger  $m=2$  complexes, which deplete into the  $m=1$  channels by  $\text{CO}_2$  loss.

### 3. Fragmentation of $[\text{Pt}_n(\text{CO}_2)_2]^-$ , $[\text{Pt}_n\text{O}(\text{CO}_2)_2]^-$ and $[\text{Pt}_n(\text{CO}_2)]^-$ Clusters



**Figure S3.** Absolute difference spectra showing the fragmentation of  $[\text{Pt}_n(\text{CO}_2)]^-$  ( $n=4$  or  $5$ ) clusters in the spectral region  $400\text{--}2100\text{ cm}^{-1}$ . For both  $n=4$  and  $n=5$  there is no enhancement into the oxide channel but an enhancement at  $1600$  and  $2000\text{ cm}^{-1}$  of the bare clusters, respectively. This indicates the loss of a complete  $\text{CO}_2$  unit. For  $n=5$  the enhancement at the frequency of the CO stretch indicates that heating the CO stretch with infrared light induces the back oxidation of the CO and the dissociation of a whole  $\text{CO}_2$  molecule, as observed previously for platinum cations.<sup>[1]</sup>

## 4. Details of the Computational Methodology Employed

To support assignment and interpretation of the experimental IR-MPD spectra, density functional theory and harmonic vibrational frequency calculations are performed using the UB3P86<sup>[2]</sup> hybrid density functional coupled with the SDD<sup>[3]</sup> basis set using the Gaussian03 and Gaussian09 suite of programs.<sup>[4]</sup> The structure search was performed using the stochastic KICK algorithm developed by Addicoat and Metha.<sup>[5]</sup> Calculations are repeated using the TPSS<sup>[6]</sup>-Def2TZVP<sup>[7]</sup> functional-basis set combination to test any functional dependence. The potential energy profile was additionally reoptimised in the PBE<sup>[8]</sup>-SDD combination.

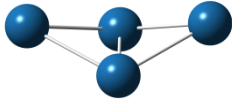
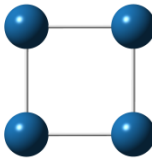
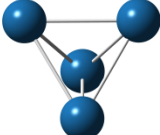
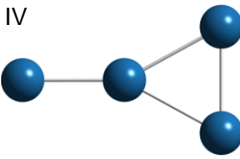
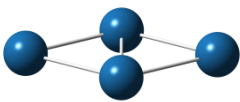
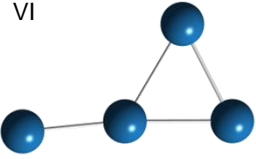
For the potential energy profile, connections between minima and transition states were verified using Intrinsic Reaction Coordinate (IRC).

The calculated energies of each structure are given relative to the putative global minimum, inclusive of zero-point energy. However energies in the potential energy profile are given relative to the  $\text{Pt}_4^- + \text{CO}_2$  asymptote.

All structures shown within the paper represent quartet spin states. See figures S4 and S5 for a comparison with the sextet spin state. All other spin states were found to lie significantly higher in energy and are therefore not expected to contribute.

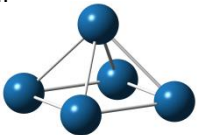

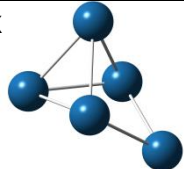


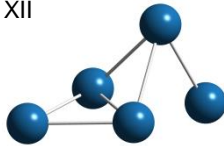
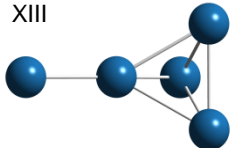
## 5. Calculated Energetically Low-Lying Structures of Pt<sub>4</sub><sup>-</sup>

**Table S1.** The calculated structures and relative energies of Pt<sub>4</sub><sup>-</sup>, where the lowest energy structure for each multiplicity is highlighted. Structures that are not found are marked with a hyphen. The lowest energy octet structure is 1.18 eV higher than the overall ground state structure.

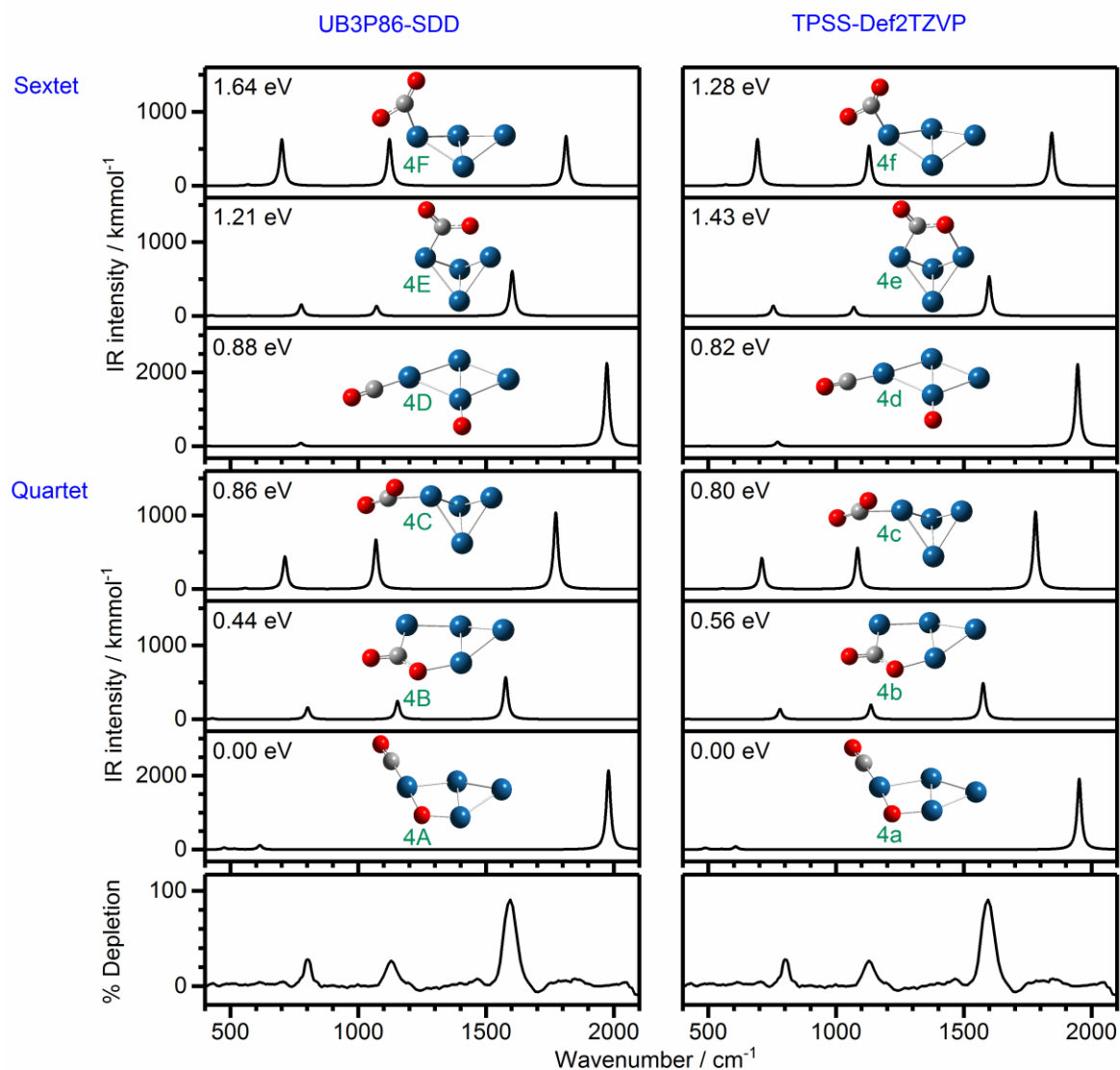
Structure Type	Doublet	Quartet	Sextet
I 	<b>0.18 eV</b>	<b>0.00 eV</b>	0.56 eV
II 	0.42 eV	0.75 eV	<b>0.26 eV</b>
III 	0.38 eV	0.34 eV	0.31 eV
IV 	0.31 eV	0.43 eV	-
V 	-	0.33 eV	0.66 eV
VI 	-	0.51 eV	0.97 eV

## 6. Calculated Energetically Low-Lying Structures of $\text{Pt}_5^-$

**Table S2.** The calculated structures and relative energies of  $\text{Pt}_5^-$ , where the lowest energy structure for each multiplicity is highlighted. Structures that are not found are marked with a hyphen.

Structure Type	Doublet	Quartet	Sextet	Octet
VII 	-	-	<b>0.00 eV</b>	<b>0.14 eV</b>
VIII 	<b>0.35 eV</b>	<b>0.09 eV</b>	0.13 eV	1.50 eV
IX 	0.39 eV	-	0.11 eV	0.75 eV
X 	-	0.57 eV	0.21 eV	-
XI 	0.38 eV	0.21 eV	-	0.68 eV
XII 	0.37 eV	0.25 eV	-	-
XIII 	0.56 eV	0.36 eV	0.72 eV	-

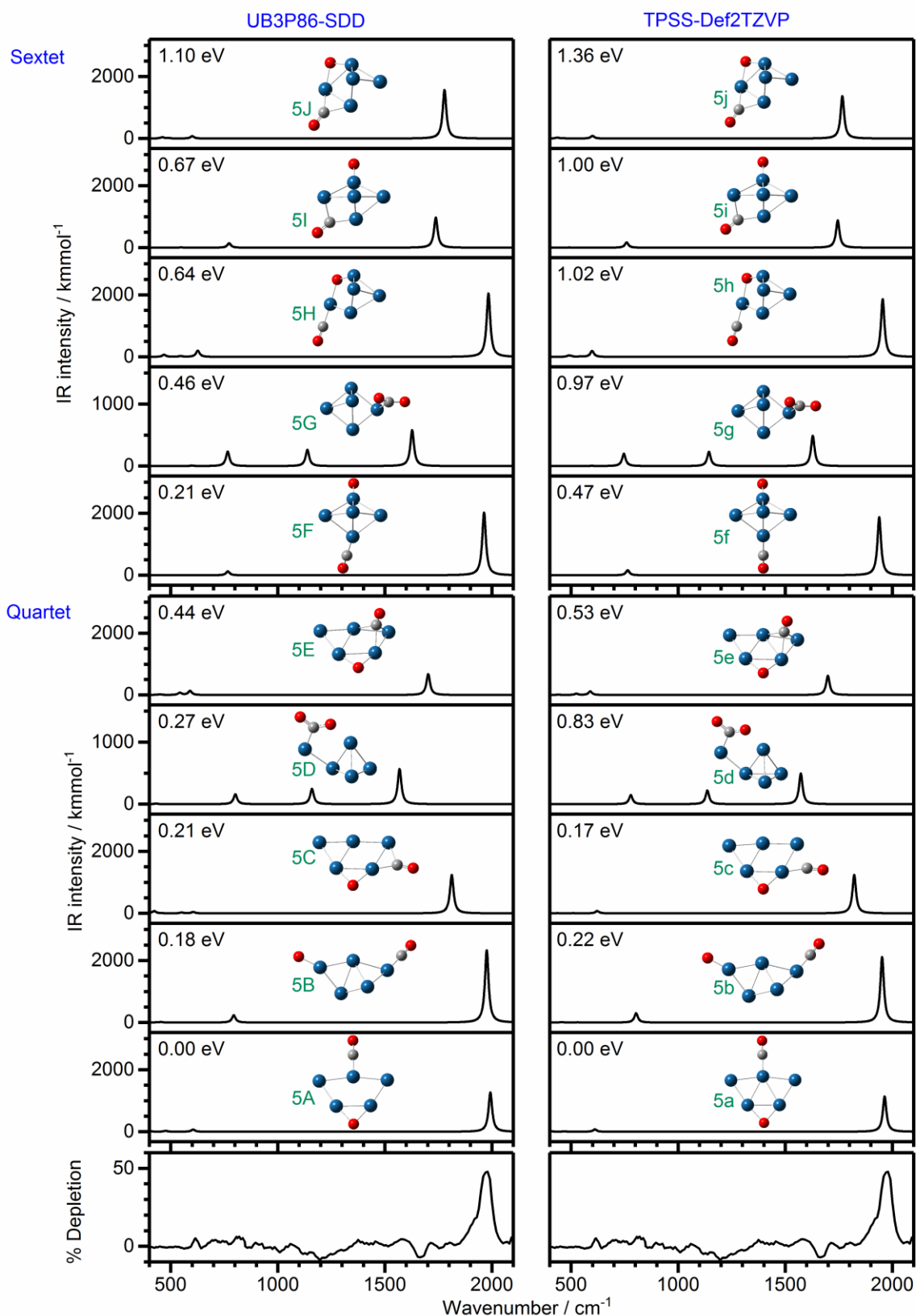
## 7. Simulated IR Spectra of Low-Lying $[\text{Pt}_4(\text{CO}_2)]^-$ Structures



**Figure S4.** Simulated IR spectra for low-lying isomers of  $[\text{Pt}_4\text{CO}_2]^-$  with different structural motifs, calculated at the UB3P86-SDD level of theory (structure 4A-F) and again at the TPSS-Def2TZVP level of theory (structure 4a-f). Structures 4A-C and 4a-c are calculated in the quartet spin state and use  $\text{Pt}_4^-$  structure I (Table S1) as a starting point. Structures 4D-F and 4d-f are calculated in the sextet spin state and use  $\text{Pt}_4^-$  structure II (Table S1) as a starting point. The relative energies are given with respect to the global minimum structure.



## 8. Simulated IR Spectra of Low-Lying $[\text{Pt}_5(\text{CO}_2)]^-$ Structures

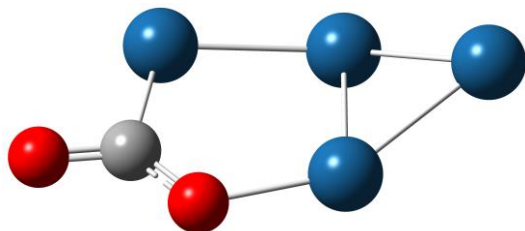


**Figure S5.** Simulated IR spectra for low-lying isomers of  $[\text{Pt}_5\text{CO}_2]^-$  with different structural motifs, calculated at the UB3P86-SDD level of theory (structure 5A-J) and again at the TPSS-Def2TZVP level of theory (structure 5a-j). Structures 5A-E and 5a-e are calculated in the quartet spin state and use  $\text{Pt}_5^-$  structure VIII (Table S2) as a starting point. Structures 5F-J and 5f-j are calculated in the sextet spin state and use  $\text{Pt}_5^-$  structure VII (Table S2) as a starting point. The relative energies are given with respect to the global minimum structure.

## 9. Details of Key Structures

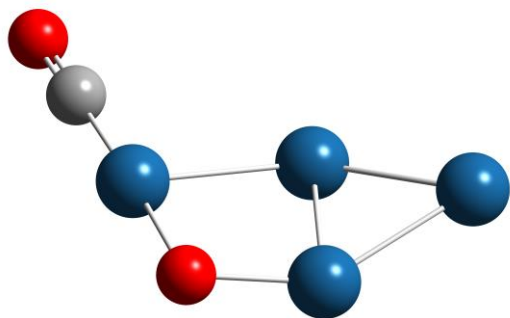
**Table S3.** Cartesian coordinates of a) the lowest energy molecularly bound minimum of  $[\text{Pt}_4\text{CO}_2]^-$ ; b) the global minimum of  $[\text{Pt}_4\text{CO}_2]^-$  and c) the global minimum of  $[\text{Pt}_5\text{CO}_2]^-$ .

a)



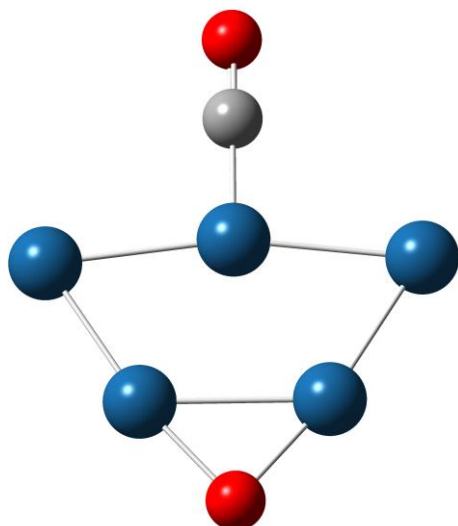
O	1.295433	-2.224364	0.039079
O	3.536529	-1.842025	-0.34509
C	2.351995	-1.45721	-0.152082
Pt	-2.340286	0.253569	-0.365939
Pt	-0.566468	-1.370384	0.2444
Pt	-0.05207	1.161831	0.405324
Pt	2.282316	0.484142	-0.240701

b)



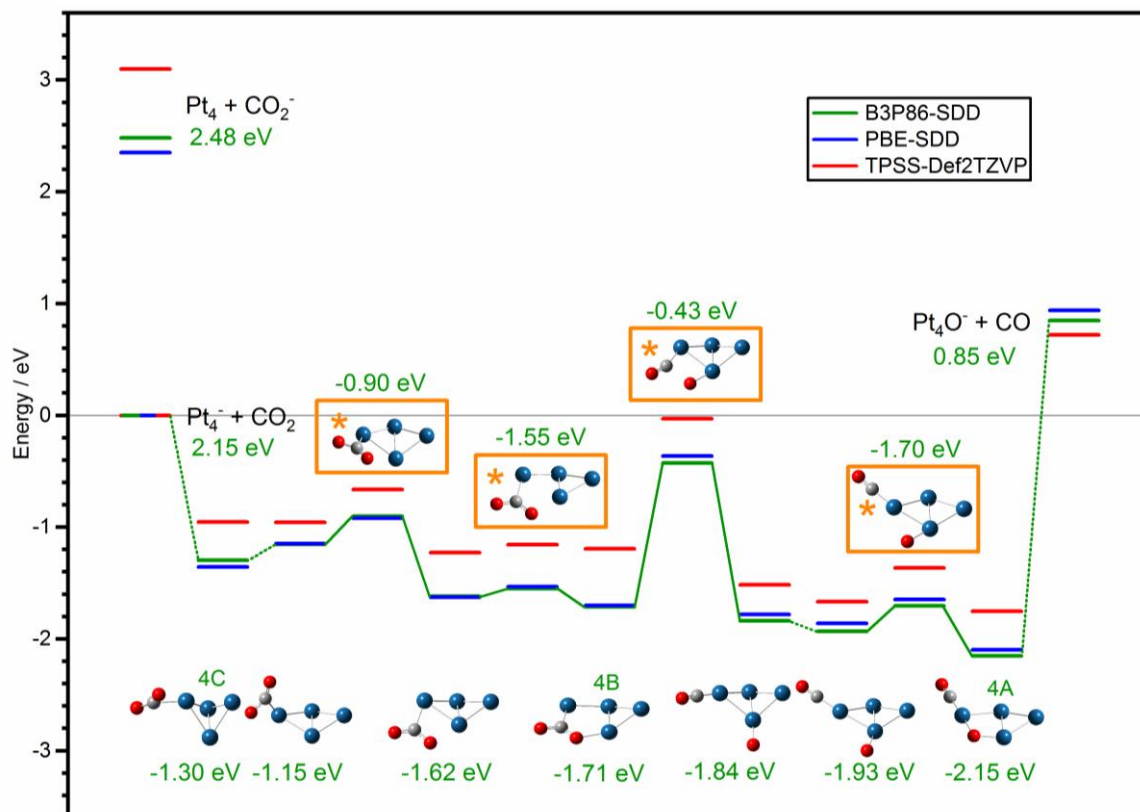
O	1.142928	1.980390	0.132840
O	4.090019	-2.060325	0.270985
C	3.354324	-1.125247	0.220992
Pt	-0.681817	1.374301	-0.156352
Pt	2.249791	0.313941	0.148882
Pt	-2.372053	-0.490504	0.263438
Pt	0.009342	-1.102983	-0.314386

c)



O	0.00062	-2.896074	0.001856
O	0.00083	4.026556	0.00005
C	-0.000366	2.840094	-0.001979
Pt	2.599215	0.713571	0.00351
Pt	1.312647	-1.391675	-0.005258
Pt	-1.310363	-1.39082	0.00458
Pt	-0.000815	1.023316	-0.001423
Pt	-2.600804	0.711192	-0.001453

## 10. Calculated $\text{Pt}_4^- + \text{CO}_2$ Reactive Potential Energy Surface



**Figure S6.** Full potential energy profile for the adsorption and dissociation of  $\text{CO}_2$  on  $\text{Pt}_4^-$  using the B3P86-SDD functional-basis set combination (green). Each minimum and transition state has been reoptimised at two other levels of theory. The energies plotted are given relative to the  $\text{Pt}_4^- + \text{CO}_2$  asymptote calculated under the relevant level of theory. The energies stated to two decimal places are using B3P86-SDD and the asterisks indicate the transition state structures. Dotted lines indicate that they have not been connected directly due to the fluxional nature of  $\text{Pt}_4^-$ .

## 11. Calculated Energetically Low-Lying Structures of $[\text{Pt}_n(\text{CO}_2)]^-$ ( $n = 1-3$ )

**Table S4.** Simulated structures for the energetically low-lying isomers of a)  $[\text{PtCO}_2]^-$ , b)  $[\text{Pt}_2\text{CO}_2]^-$ , and c)  $[\text{Pt}_3\text{CO}_2]^-$ . The UB3P86-SDD, functional-basis set combination was used. Energies are given relative to their putative global minimum.

a)	0.00 eV	0.65 eV	1.95 eV

b)	0.00 eV	0.06 eV	0.15 eV	0.40 eV	0.66 eV

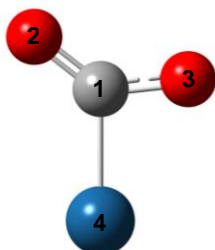
c)	0.00 eV	0.13 eV	0.19 eV	0.30 eV	0.31 eV	0.65 eV
	0.75 eV	0.75 eV	0.83 eV	0.90 eV	0.92 eV	0.95 eV

## 12. Charge Distribution Analysis of Key Structures

**Table S5.** Atomic charge analysis for the molecularly adsorbed isomers of CO<sub>2</sub> on Pt<sub>n</sub> (n=1-5). ΔE is given relative to the ground state isomer for that cluster size. Atomic charges are calculated using both natural population analysis (NPA) and Mulliken analysis.

### Monomer

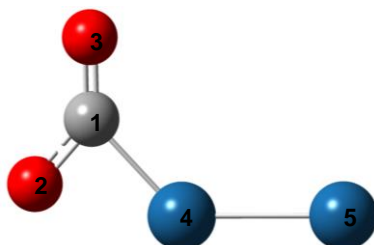
a)  
ΔE = 0.65 eV



		NPA	Mulliken
1	C	0.70	0.11
2	O	-0.68	-0.34
3	O	-0.68	-0.37
	<b>CO<sub>2</sub></b>	<b>-0.66</b>	<b>-0.60</b>
4	Pt	-0.34	-0.40

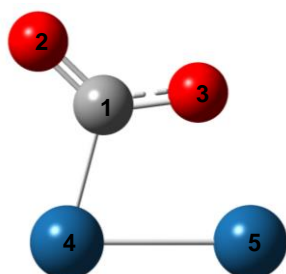
### Dimer

b)  
ΔE = 0.40 eV



		NPA	Mulliken
1	C	0.73	0.14
2	O	-0.66	-0.34
3	O	-0.62	-0.28
	<b>CO<sub>2</sub></b>	<b>-0.55</b>	<b>-0.48</b>
4	Pt	-0.03	0.02
5	Pt	-0.42	-0.54

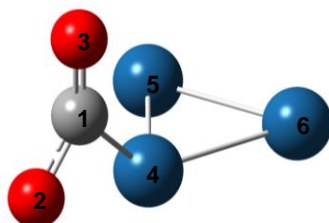
c)  
ΔE = 0.66 eV



		NPA	Mulliken
1	C	0.70	0.17
2	O	-0.66	-0.34
3	O	-0.72	-0.39
	<b>CO<sub>2</sub></b>	<b>-0.68</b>	<b>-0.55</b>
4	Pt	-0.27	-0.34
5	Pt	-0.05	-0.11

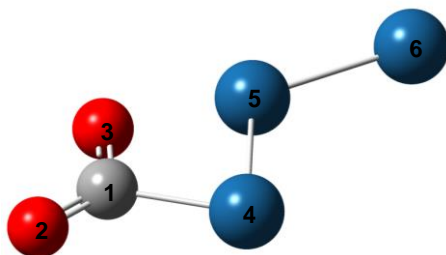
### Trimer

d)  
ΔE = 0.65 eV



		NPA	Mulliken
1	C	0.74	0.16
2	O	-0.65	-0.33
3	O	-0.61	-0.28
	<b>CO<sub>2</sub></b>	<b>-0.52</b>	<b>-0.45</b>
4	Pt	-0.05	-0.01
5	Pt	-0.16	-0.18
6	Pt	-0.27	-0.35

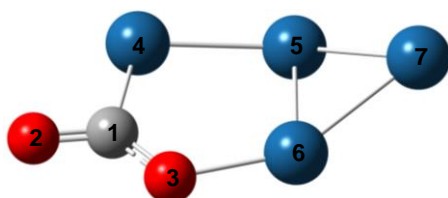
e)  
 $\Delta E = 0.75 \text{ eV}$



		NPA	Mulliken
1	C	0.69	0.16
2	O	-0.64	-0.31
3	O	-0.69	-0.36
	<b>CO<sub>2</sub></b>	<b>-0.64</b>	<b>-0.50</b>
4	Pt	0.02	-0.19
5	Pt	0.01	0.11
6	Pt	-0.40	-0.42

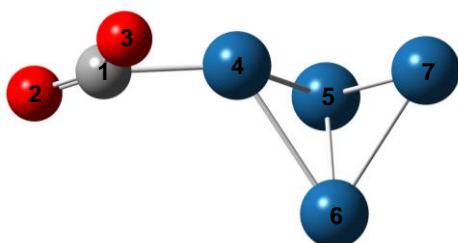
Tetramer

f)  
 $\Delta E = 0.44 \text{ eV}$



		NPA	Mulliken
1	C	0.73	0.17
2	O	-0.63	-0.31
3	O	-0.71	-0.41
	<b>CO<sub>2</sub></b>	<b>-0.61</b>	<b>-0.56</b>
4	Pt	-0.11	-0.11
5	Pt	-0.20	-0.08
6	Pt	0.18	0.08
7	Pt	-0.26	-0.34

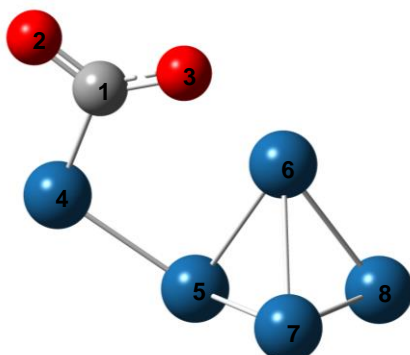
g)  
 $\Delta E = 0.86 \text{ eV}$



		NPA	Mulliken
1	C	0.72	0.16
2	O	-0.62	-0.29
3	O	-0.64	-0.34
	<b>CO<sub>2</sub></b>	<b>-0.54</b>	<b>-0.46</b>
4	Pt	-0.05	0.10
5	Pt	-0.21	-0.3
6	Pt	-0.04	-0.14
7	Pt	-0.16	-0.21

Pentamer

h)  
 $\Delta E = 0.27 \text{ eV}$



		NPA	Mulliken
1	C	0.74	0.16
2	O	-0.64	-0.32
3	O	-0.71	-0.41
	<b>CO<sub>2</sub></b>	<b>-0.62</b>	<b>-0.56</b>
4	Pt	-0.13	-0.06
5	Pt	-0.27	-0.09
6	Pt	0.12	0.06
7	Pt	0.07	-0.12
8	Pt	-0.18	-0.23

- [1] A. C. Hermes, S. M. Hamilton, G. A. Cooper, C. Kerpál, D. J. Harding, G. Meijer, A. Fielicke, S. R. Mackenzie, *Faraday Discuss.* **2012**, *157*, 213.
- [2] a) J. P. Perdew, *Phys. Rev. B* **1986**, *33*, 8822; b) A. D. Becke, *J. Chem. Phys.* **1993**, *98*, 5648.
- [3] T. H. Dunning, *J. Chem. Phys.* **1970**, *53*, 2823.
- [4] a) M. J. Frisch, *et al.*, *Gaussian 09*, Gaussian, Inc., Wallingford CT, **2009**; b) M. J. Frisch, *et al.*, *Gaussian 03*, Gaussian, Inc., Wallingford CT, **2004**.
- [5] M. A. Addicoat, G. F. Metha, *J. Comput. Chem.* **2009**, *30*, 57.
- [6] a) V. K. Staroverov, G. E. Scuseria, J. Tao, J. P. Perdew, *J. Chem. Phys.* **2003**, *119*, 12129; b) J. Tao, J. P. Perdew, V. K. Staroverov, G. E. Scuseria, *Phys. Rev. Lett.* **2003**, *91*, 146401.
- [7] a) F. Weigend, *Phys. Chem. Chem. Phys.* **2006**, *8*, 1057; b) F. Weigend, R. Ahlrichs, *Phys. Chem. Chem. Phys.* **2005**, *7*, 3297.
- [8] J. P. Perdew, M. Ernzerhof, K. Burke, *J. Chem. Phys.* **1996**, *105*, 9982.